# Catalysis Science & Technology



PAPER

View Article Online

View Journal | View Issue



**Cite this:** *Catal. Sci. Technol.*, 2025, **15**, 5327

Received 3rd June 2025, Accepted 11th August 2025

DOI: 10.1039/d5cy00662g

rsc.li/catalysis

# Role of base in CO<sub>2</sub> hydrogenation to formate over a Ru<sup>(III)</sup> solid micellar catalyst

Catarina M. De Brito Mendes, D<sup>a</sup> Javiera Rubio, Francisca Rebelo, Sara Santos, D<sup>a</sup> Jan Öner, Vitaly V. Ordomsky D<sup>c</sup> and Mark Saeys D\*<sup>a</sup>

The catalytic conversion of  $CO_2$  to formate is generally performed under basic conditions. While the specific role of amines may not always be clearly defined, they have been the preferred additives to enhance activity and conversion. In this work, we demonstrate that during  $CO_2$  hydrogenation to formate over a  $Ru^{(III)}$  solid micellar catalyst, the base acts as a promoter by improving the sluggish heterolytic  $H_2$  dissociation. Kinetic experiments revealed that it is crucial to direct  $CO_2$  speciation towards bicarbonate to ensure formate generation, and that there is a strong dependence of the hydrogenation rate on  $H_2$  and TEA availability.  $H_2$ - $D_2$  isotope scrambling showed a fourfold increase in the presence of the base. Screening of different bases evidenced the unique promoting effect of TEA.

# 1. Introduction

The catalytic transformation of CO<sub>2</sub> to formate/formic acid is gaining attention due to the potential of formate salts/formic acid for reversible hydrogen storage. The synthesis of formic acid from CO<sub>2</sub> and H<sub>2</sub> is endergonic in the gas phase, but the reaction becomes thermodynamically favorable in aqueous medium due to solvation effects. Stoichiometric amounts of bases are typically added as co-reagents to promote the stabilization of formic acid as formate salts or adducts. N-containing organic bases, used as reaction additives, and amine-related functional groups, incorporated as ligands in molecular catalysts, promote CO<sub>2</sub> reduction by acting as proton shuttles, capturing CO<sub>2</sub>, and providing electronic stabilization to reaction intermediates.

Proton shuttles are important in  $CO_2$  hydrogenation to formate, as they facilitate  $H_2$  heterolytic cleavage into a hydride and a proton. The hydride reacts with  $CO_2$  to produce formate, while the proton needs to be efficiently transferred to a base to close the catalytic cycle. Amines readily accept a proton, forming ammonium. Filonenko *et al.* attributed the high hydrogenation rate over a Ru PNP-pincer catalyst in a mixture of *N,N*-dimethylformamide (DMF) and 1,8-diazabicyclo[5.4.0]undec-7-ene (DBU) to the amine-assisted Ru–H bond formation *via* heterolytic dissociation of a coordinated  $H_2$  molecule.  $^{7,8}$  In their

study, activity was further enhanced by increasing  $H_2$  partial pressure. Rawat *et al.* demonstrated that the heterolytic  $H_2$  cleavage and hydride transfer over a series of Fe complexes improved due to the presence of an outer-sphere pendant amine.<sup>9</sup>

Amines have been employed as  $CO_2$  trapping agents in reduction reactions over homogeneous catalysts due to their  $CO_2$ -capturing ability. In the presence of water, primary and secondary amines (RNH $_2$  and R $_2$ NH) react with  $CO_2$  to form carbamates (RNHCOO $^-$  and R $_2$ NCOO $^-$ ) which can hydrolyze to produce bicarbonate (HCO $_3$  $^-$ ) and protonated amines (RNH $_3$  $^+$  and R $_2$ NH $_2$  $^+$ ). Tertiary amines (R $_3$ N) directly form HCO $_3$  $^-$  and protonated tertiary amines (R $_3$ NH $^+$ ). In organic solvents, where reactants and products have only one possible form, alkaline aqueous solutions involve multiple equilibria, with reactive species and products varying based on amine type and concentration, pH, temperature and  $CO_2$  partial pressure.  $^{11,12}$ 

High CO<sub>2</sub> conversions have been reported over homogeneous catalysts in the presence of amines, with several examples in the literature displaying advancements in catalyst and process development. Compared to homogeneous catalysts, heterogeneous catalysts own several advantages for large-scale application in continuous flow, including improved catalyst stability and lower production costs. Single-site catalysts are especially promising for CO<sub>2</sub> hydrogenation to formate due to their resemblance to homogeneous systems: well-defined active sites, high activity and selectivity.

Ru<sup>(III)</sup>@MCM is the first example of a SOlid MICellar (SOMIC) catalyst, consisting of Ru<sup>(III)</sup> single sites incorporated into the walls of MCM-41 *via* Ru-O-Si bonds, and stabilized by a cetyltrimethylammonium (CTA<sup>+</sup>). The presence of the CTA<sup>+</sup>

<sup>&</sup>lt;sup>a</sup>Laboratory for Chemical Technology, Department of Materials, Textiles and Chemical Engineering, Ghent University, Technologiepark 125, 9052 Ghent, Belgium. E-mail: mark.saeys@ugent.be

b Chemical Engineering Department, Instituto Superior Técnico, Universidade de Lisboa. Av. Rovisco Pais. 1049-001 Lisbon. Portugal

<sup>&</sup>lt;sup>c</sup> Univ. Lille, CNRS, Centrale Lille, ENSCL, Univ. Artois, UMR 8181 – UCCS – Unité de Catalyse et Chimie du Solide, F-59000 Lille, France

molecules prevents sintering and creates an apolar environment in the pores, favoring the concentration of nonpolar reactants and intermediates while excluding bulk water. 17,18 The Ru(III) active sites maintain a local environment where water can still interact through coordination or hydrogen bonding, ensuring their accessibility to aqueous-phase reactants.

At 90 °C and 50 bar, a turnover frequency (TOF) of 182 h<sup>-1</sup> and a formate concentration of 1 mol L<sup>-1</sup> after 15 h was reached in aqueous medium and in the presence of TEA over Ru(III) (a) MCM. Catalyst activity and selectivity was maintained over four consecutive CO<sub>2</sub> hydrogenation cycles. 18 DFT modelling suggests that the reaction proceeds via heterolytic splitting of H<sub>2</sub>, forming a Ru-H species, followed by hydride transfer to CO<sub>2</sub>. H<sub>2</sub> activation is the rate-determining step of the reaction and the Ru-H complex is identified as the resting state of the catalyst. The role of base was not explicitly included in the reaction path, but it was hypothesized that the heterolytic H2 dissociation could happen over (O)3SiO, OH<sup>-</sup>, HCO<sub>2</sub><sup>-</sup>, HCO<sub>3</sub><sup>-</sup> or TEA.

In this work, we investigate the reaction kinetics of CO2 hydrogenation to formate over Ru(III) (a) MCM, focusing on the influence and mechanistic role of the base. Combining the study of the dependence of formate concentration on reaction conditions and H2-D2 isotope scrambling, we evaluate the role of pH and CO2 speciation in the reaction medium, the influence of H2 partial pressure and TEA concentration on the formate production rate. The performance of a selection of different solvents and bases is evaluated and compared.

# 2. Experimental

#### 2.1 Chemicals

Hexadecyltrimethylammonium bromide (CTAB, C<sub>19</sub>H<sub>42</sub>BrN, ≥98%), ruthenium chloride (RuCl<sub>3</sub>, Ru content 45–55%), ammonium hydroxide solution (NH<sub>4</sub>OH, ACS reagent 28-30% NH<sub>3</sub> basis), tetraethyl orthosilicate (TEOS, SiC<sub>8</sub>H<sub>20</sub>O<sub>4</sub>, reagent grade 98%), triethylamine (TEA,  $C_6H_{15}N$ ,  $\geq 99\%$ ), tripropylamine (TPA,  $C_9H_{21}N$ ,  $\geq 98\%$ ), triethanolamine (TEOA,  $C_6H_{15}NO_3$ ,  $\geq$ 98%), N,N-diisopropylethylamine (DIPEA, C<sub>8</sub>H<sub>19</sub>N,  $\geq$ 99%), propylamine (PA, C<sub>3</sub>H<sub>9</sub>N, ≥98%), and morpholine (Mor,  $C_4H_9NO$ ,  $\geq 99\%$ ), dimethyl sulfoxide (DMSO, (CH<sub>3</sub>)<sub>2</sub>SO,  $\geq 99\%$ ) and methanol (MeOH, CH<sub>3</sub>OH, ≥99.8%) were purchased from Merck Chemicals. Ethanol (EtOH, C2H5OH, denaturated with Eurodenaturant) was supplied by Chem Lab. Water was deionized using a Millipore system. H2, CO2 and Ar were purchased from Air Liquide and D2 was purchased from Eurisotop. All chemicals were used without further purification.

#### 2.2 Catalyst synthesis

Ru(III) (a) MCM was prepared according to the procedure described by Wang et al.18 0.5 g of hexadecyltrimethylammonium bromide (CTAB) powder was added to 96 mL of deionized water and 34 mL of ethanol under stirring at 250 rpm for 30 minutes, until a fully transparent solution was obtained. Then, 0.09 g of ruthenium(III) chloride was added to the mixture and stirred at

650 rpm for 20 minutes to ensure RuCl<sub>3</sub> was fully dissolved. Next, 10 mL of aqueous ammonium hydroxide solution (NH<sub>4</sub>OH) was added, followed by the dropwise addition of 2 mL of tetraethyl orthosilicate (TEOS). The resulting solution was stirred for three hours at room temperature. Approximately 1 g of solid product was collected through vacuum filtration, washed with distilled water until the filtrate attained a neutral pH, and finally dried overnight at room temperature.

Ru(III) (a) Mic is the homogeneous counterpart of Ru(III) (a)MCM. 0.5 g of CTAB powder was added to 96 mL of deionized water and 34 mL of ethanol. The mixture was stirred at 250 rpm for 30 minutes until a fully transparent solution was obtained. Then, 0.09 g of ruthenium(III) chloride was added to the mixture and stirred at 650 rpm for 20 minutes, ensuring complete dissolution of RuCl3. No TEOS was introduced.

#### 2.3 Catalytic tests

Hydrogenation reactions were performed in a 45 mL stainless steel pressure reactor manufactured by Parr Instrument Company, with a PTFE inner chamber. During reaction, the vessel was placed in an aluminum support placed on a ceramic hot plate stirrer (IKA C-MAG HS7). Temperature was controlled using an electronic contact thermometer (IKA ETS-D5) placed in the aluminum support (Fig. S1, SI).

In a standard procedure, the vessel was initially filled with water, base, fresh catalyst and a magnetic stirrer. Then, the reactor was sealed, purged with CO2, pressurized with the gaseous reactants and gradually heated to the desired reaction temperature for 30 minutes. After reaction, the vessel was cooled to room temperature, the pressure released and the gas phase analyzed via gas chromatography (GC). The liquid product was separated from the catalyst using a syringe filter. Quantitative analysis of the formate concentration in the liquid product ( $C_{\text{HCOO}}$ ) was performed via <sup>1</sup>H NMR using a Spinsolve 80 MHz phosphorous benchtop NMR spectrometer from Magritek and TSP-d<sub>4</sub> as internal standard (Fig. S2, SI). The standard deviation was calculated based on eqn (1), in which  $C_{\text{HCOO-},i}$  is the individual formate concentration measured from each sample,  $\overline{C_{\text{HCOO}^-}}$  is the average of the concentrations measured for each reaction and n is the total number of measurements.

Standard deviation = 
$$\sqrt{\frac{\sum (C_{\text{HCOO}^-,i} - \overline{C_{\text{HCOO}^-}})^2}{(n-1)}}$$
 (1)

The turnover frequency (TOF) and base conversion were calculated as defined in eqn (2) and (3), respectively.

TOF 
$$(h^{-1}) = \frac{C_{\text{HCOO}^-} \times V}{n_{\text{Ru}} \times t}$$
 (2)

$$X_{\text{base}}(\%) = \frac{n_{\text{HCOO}^-}}{n_{\text{base}}^0} \tag{3}$$

where V is the volume of the reaction product,  $n_{Ru}$  is the amount of Ru (mol) in the catalyst used, t is the reaction time

(h),  $n_{\rm HCOO^-}$  is the amount of formate (mol) in the reaction product, and  $n_{\rm base}^0$  is the amount of base (mol) added to the reaction feed.

#### 2.4 H<sub>2</sub>-D<sub>2</sub> isotope scrambling

H<sub>2</sub>-D<sub>2</sub> exchange reactions were performed using the same autoclave employed for the catalytic tests. Prior to each reaction, water, base and fresh catalyst were added to the autoclave. The reactor was sealed, pressurized with H2 and D<sub>2</sub> with a ratio 1:1, and heated to the reaction temperature for 15 min. After reaction, the vessel was cooled to room temperature and connected to a mass spectrometer (MS) for off-line gas analysis. The gas released from the reactor was continuously diluted with argon (Ar) as a carrier gas in a flow line, ensuring a flow rate of 50 Nml min<sup>-1</sup>. This diluted gas mixture was analyzed using Mass Spectrometry (MS) to monitor the composition until all the gas content was released from the autoclave. During the analysis, the relative intensities of H<sub>2</sub>, D<sub>2</sub>, and HD were quantified by calculating the signal ratios H<sub>2</sub>/Ar, D<sub>2</sub>/Ar, and HD/Ar. These ratios were derived from the raw MS signals recorded throughout the analysis period, providing a comparative measure of each gas component relative to the inert Ar reference.

# 3. Results and discussion

#### 3.1 Kinetic insights

The effect of reaction time on formate concentration, catalyst activity, and TEA conversion was evaluated in a range from 3 to 20 h. The maximum formate concentration reached is 1.23 mol L<sup>-1</sup> after 20 h (Table 1, entry 6), aligning with the catalyst performance previously reported. 18 Gas chromatography analysis confirmed the absence of CO and CH<sub>4</sub> after reaction. Catalyst productivity peaks at 2.6 g HCOO per gcat. h-1 (TOF = 214 h<sup>-1</sup>) after 10 h (Table 1, entry 4). The pH remains constant throughout the reaction, and formate production increases linearly during the first ten hours. As the reaction progresses, activity slows down at formate concentrations higher than 1 mol L<sup>-1</sup> (Table 1, entries 4 to 6), near full TEA conversion. To guarantee the collection of kinetic data throughout our study, a reaction time of 4 h ( $X_{\text{TEA}} \sim 24\%$ , Table 1) was selected to study the dependence of formate concentration on the reaction conditions.

Table 1 Effect of reaction time on formate concentration, catalyst activity and TEA conversion. Conditions: 3.1  $\mu$ mol Ru, 9 mmol TEA, 6 mL H<sub>2</sub>O, 30 bar H<sub>2</sub>, 20 bar CO<sub>2</sub>, 90 °C

Entry	Reaction time (h)	[HCOO <sup>-</sup> ] (mol L <sup>-1</sup> )	TOF (h1)	$X_{\mathrm{TEA}}$ (%)
1	3	0.08	56	5.9
2	4	0.31	158	24.2
3	5	0.42	174	30.5
4	10	1.03	214	75.9
5	15	1.09	162	85.4
6	20	1.23	137	95.8

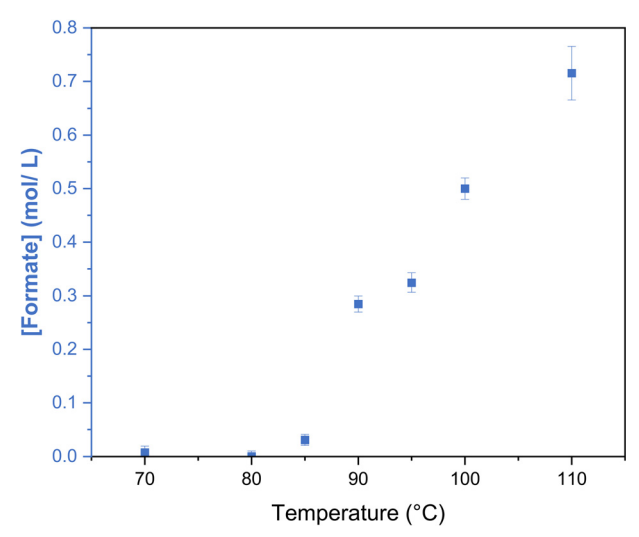


Fig. 1 Effect of temperature on formate concentration. Conditions:  $3.1 \, \mu mol \, Ru$ , 9 mmol TEA, 6 mL H<sub>2</sub>O, 30 bar H<sub>2</sub>, 20 bar CO<sub>2</sub>, 4 h.

The catalytic hydrogenation of CO<sub>2</sub> over Ru<sup>(III)</sup>@MCM in the liquid phase requires the transfer of CO<sub>2</sub> and H<sub>2</sub> from the gas to the liquid phase, from the liquid phase to the external surface of the catalyst and finally to and within the pores of the catalyst. A study of the effect of stirring speed indicates no external mass transfer limitations above 750 rpm (Fig. S3, SI).

Varying the reaction temperature from 70 to 110 °C (Fig. 1) showed that formate production becomes measurable at 85 °C, and that an increase in the temperature improves  $CO_2$  hydrogenation. The apparent activation energy ( $E_{app}$ ) is 56 kJ mol<sup>-1</sup> (Fig. S4, SI).

The dependence of formate concentration on the gaseous reactants partial pressure was investigated. A limited effect of  $CO_2$  partial pressure is found (Fig. S5, SI). In contrast, there is a significant influence of  $H_2$  partial pressure on the product concentration. An increase from to 10 to 30 bar leads to a tenfold increase of formate concentration (0.31 mol  $L^{-1}$ , Fig. 2) in the reaction product. A quasi-second order in  $H_2$  is calculated (Fig. S6, SI), indicating that  $H_2$  adsorption and activation are kinetically relevant.

The reaction was also studied at different TEA concentrations in the feed ( $X_{\rm TEA} < 25\%$ ). In water, a very low concentration of formic acid is obtained (Fig. S7, SI). Formate concentration increases linearly from 0.05 to 0.35 mol L<sup>-1</sup> when the TEA concentration in the aqueous reaction feed is varied from 0.6 to 1.5 mol L<sup>-1</sup> (Fig. 3), all at low TEA conversion ( $X_{\rm TEA} < 25\%$ ). When the concentration of TEA in the reaction feed exceeds 1.5 mol L<sup>-1</sup>, catalyst performance drops (Fig. 3). Extending the reaction time from 4 h to 15 h shows a similar effect (Fig. S8, SI).

The decrease in the  $Ru^{(III)}$ @MCM performance at higher TEA concentrations can be linked to a change in the pH of the liquid phase. Within the pH range of 8–9, bicarbonate ( $HCO_3^-$ ) is the main form of carbon in solution (Fig. S9, SI). In a more alkaline medium, carbonate ( $CO_3^{-2}$ ) becomes the dominant

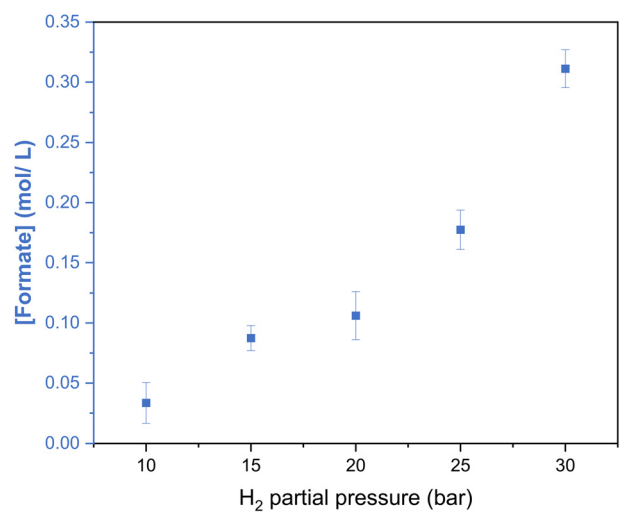


Fig. 2 Dependence of the formate concentration on H<sub>2</sub> partial pressure. Conditions: 3.1 µmol Ru, 9 mmol TEA, 6 mL H<sub>2</sub>O, 20 bar CO<sub>2</sub>, 90 °C, 4 h.

species (Fig. S9, SI). KHCO<sub>3</sub> was directly hydrogenated at pH 12 in the absence of CO<sub>2</sub> (entry 2, Table S1, SI, Fig. S10, SI), resulting in no formate production. However, when KHCO3 hydrogenation was performed under CO2 pressure at pH 8 (entry 4, Table S1, SI, Fig. S11, SI), the formate concentration increased significantly, surpassing that of the standard TEAbased system (0.31 mol L<sup>-1</sup>, entry 1, Table S1, SI). In contrast, performing CO2 hydrogenation at pH 8 in the presence of KHCO3 but without TEA led to a notably lower formate concentration (entry 5, Table S1, SI, Fig. S12, SI), indicating that maintaining the pH at 8 alone is insufficient for high catalytic activity. Direct hydrogenation of K<sub>2</sub>CO<sub>3</sub> at pH 13 (entries 6 to 8, Table S1, SI, Fig. S13 and S14, SI) does not yield formate. CO<sub>2</sub> hydrogenation in the presence of K<sub>2</sub>CO<sub>3</sub> generates 0.26 mol L<sup>-1</sup> of formate (entry 9, Table S1, SI, Fig. S15, SI), highlighting that K<sub>2</sub>CO<sub>3</sub> can serve as a base in the reaction.

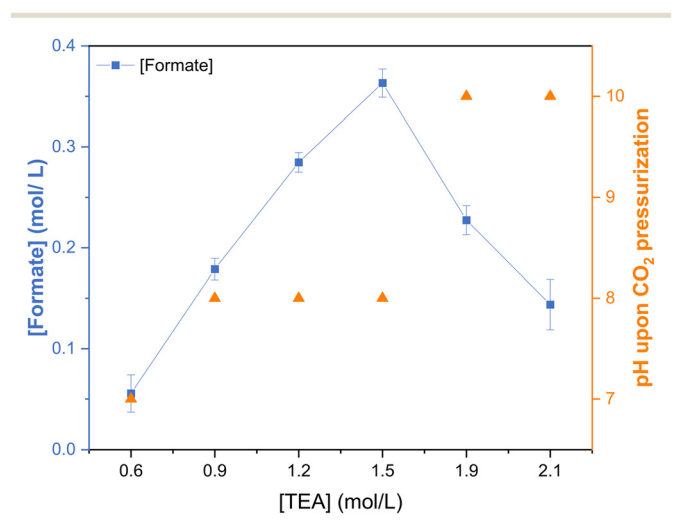


Fig. 3 Dependence of the formate concentration on the amount of TEA in the liquid reaction feed and pH upon CO<sub>2</sub> pressurization. Conditions: 3.1 µmol Ru, 6 mL H<sub>2</sub>O, 30 bar H<sub>2</sub>, 20 bar CO<sub>2</sub>, 90 °C, 4 h.

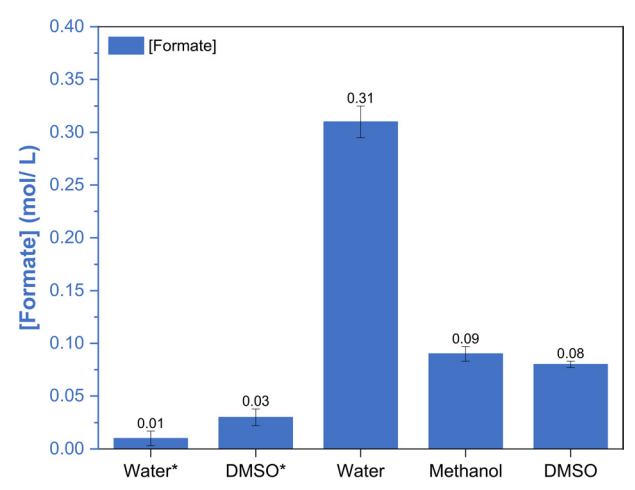


Fig. 4 Performance of Ru<sup>(III)</sup>@MCM for CO<sub>2</sub> hydrogenation to formic acid/formate in different solvents. Conditions: 3.1 µmol Ru, no TEA\* or 9 mmol, 6 mL solvent, 30 bar H<sub>2</sub>, 20 bar CO<sub>2</sub>, 90 °C, 4 h.

These results suggest that at high TEA concentration or during the direct hydrogenation of KHCO3 and K2CO3 the reaction does not proceed because the alkalinity of the medium favors the formation of CO<sub>3</sub><sup>2-</sup> over HCO<sub>3</sub><sup>-</sup>. In the presence of CO2, the pH decreases (Fig. 3, Table S2, SI), shifting the equilibrium towards HCO<sub>3</sub>. Keeping the pH of the reaction medium in the range 8-9 to maintain HCO<sub>3</sub> as the predominant species in solution seems crucial for formate synthesis over Ru(III) (a)MCM (Fig. 3).

As the choice of solvent can impact both the reaction mechanism,19 thermodynamics and catalytic  $CO_2$ hydrogenation over Ru(III)@MCM was further studied in DMSO and in methanol (Table S3, SI). Fig. 4 shows that in the absence of a base, the performance of Ru(III) (a) MCM in DMSO is similar to the one observed in water. The group of Leitner reported that DMSO stabilizes HCOOH by hydrogen bonding.<sup>6</sup> Our results demonstrate that replacing water and TEA by a solvent to promote formic acid stabilization did not lead to a higher formate concentration in our system (Fig. 4). Performing the reaction in MeOH and DMSO in the presence of TEA generated formate concentrations three times lower (approximately 0.1 mol L<sup>-1</sup>) than in aqueous medium (Fig. 4). Similarly, gradually increasing the amount of MeOH and DMSO in mixtures with water did not lead to improved performance (Tables S4 and S5, SI). In aqueous environments, TEA reacts with CO2 to produce HCO<sub>3</sub>. In non-aqueous solvents such as methanol or DMSO, CO<sub>2</sub> interaction with tertiary amines is limited.<sup>20</sup>

#### 3.2 Role of the base

The quasi-second order in H2 (Fig. S6, SI) and the first order in TEA concentration (Fig. 3) suggest that the tertiary amine is involved in H2 activation. To investigate the involvement of TEA in the heterolytic H<sub>2</sub> cleavage step during the CO<sub>2</sub> hydrogenation to formate, a set of three H2-D2 isotope scrambling experiments was carried out (Table 2). H2-D2 scrambling involves exposing hydrogen molecules to a

**Table 2** Summary of reaction conditions for  $H_2$ – $D_2$  isotope scrambling experiments and ratios between the MS raw signals of  $H_2$ ,  $D_2$ , HD and Ar after reaction. Reaction conditions: 4 bar  $H_2$ , 4 bar  $H_2$ 0, 50 °C, 1 h, analysis conditions: total flow of 50 mL min<sup>-1</sup> fed to the MS (90% Ar)

	Ru (µmol)	TEA	Ratio of	Ratio of the MS signals		
Entry		(mmol)	H <sub>2</sub> /Ar	$D_2/Ar$	HD/Ar	
1	0	0	0.59	0.19	0.01	
2	3.1	0	0.60	0.17	0.08	
3	3.1	1.4	0.28	0.10	0.30	

catalyst under specific conditions, allowing for the exchange of hydrogen atoms with deuterium atoms. Breaking of H–H bonds and the incorporation of deuterium atoms leads to the appearance of HD as a reaction product. By monitoring the extent of HD in the reaction products, conclusions about the catalyst's capacity to dissociate  $\rm H_2$  can be drawn as well as the involvement of the base.

Fig. S16, SI shows the mass spectrometer signals of  $H_2$ ,  $D_2$ , HD and  $H_2O$  during the off-line analysis of the autoclave gas content, after dilution in Ar. In the absence of both the catalyst and base, only a negligible amount of HD is formed (Table 2, entry 1). Introducing Ru<sup>(III)</sup>@MCM (Table 2, entry 2) results in an eightfold increase in the HD/Ar ratio, demonstrating the catalyst's critical role in activating  $H_2$  and facilitating hydrogenation. When TEA is added to the system (Table 2, entry 3), the HD/Ar ratio increases another fourfold. The combined presence of Ru<sup>(III)</sup>@MCM and TEA creates a synergistic effect, significantly boosting HD production and supporting the hypothesis that the base modifies the reaction mechanism.

To further confirm the involvement of TEA in  $\rm H_2$  dissociation,  $^1H$  NMR spectroscopy was conducted using the homogeneous parent complex of the Ru SOMIC catalyst, Ru<sup>(III)</sup>@Mic. Upon pressurization with  $\rm H_2$  and heating at 50 °C for 1.5 hours, distinct changes were observed in the chemical shifts of TEA (Fig. S17, SI (d)) compared to control samples lacking  $\rm H_2$  (Fig. S17, SI (c)) or Ru<sup>(III)</sup>@Mic (Fig. S17, SI (e) and (f)). Notably, the CH $_2$  resonance of TEA shifted downfield from 2.53 ppm (Fig. S17, SI (c)) to 2.78 ppm under reaction conditions (Fig. S17, SI (d)), indicating a change in the electronic environment around the nitrogen atom consistent with protonation.  $^{21}$ 

The proposed pathway for CO<sub>2</sub> hydrogenation in the presence of TEA is illustrated in Fig. 5. The first step concerns H<sub>2</sub> adsorption on the Ru active center. The formation of intermediate 2 (**Int 2**) is followed by TEA-assisted H<sub>2</sub> heterolytic dissociation *via* transition state 1 (**TS 1**), leading to the generation of a Ru hydride species and triethylammonium (**Int 3**). In the next step, the hydride is transferred to CO<sub>2</sub> (**TS 2**), which exists in dynamic equilibrium with HCO<sub>3</sub><sup>-</sup> under basic conditions. The catalytic cycle is closed by formate (**Int 4**) removal from the active site aided by triethylammonium.

The reaction involves the transport of key components—H<sub>2</sub>, CO<sub>2</sub>, and the amine—through the apolar medium formed by the CTA<sup>+</sup> surfactant within the pores of the Ru<sup>(III)</sup>@MCM structure. The apolar environment within these pores plays a critical role in mediating the interaction of the reactants with the catalytic active sites. Effective base-mediated catalysis depends on the amine's basicity and ability to partition into the nonpolar pore environment, and subsequently interact with the

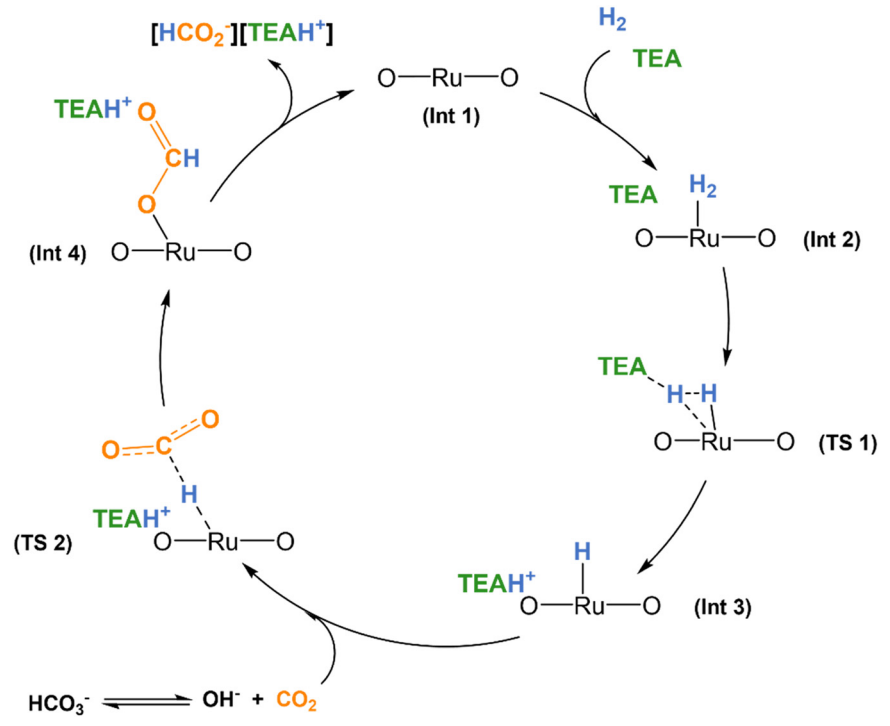
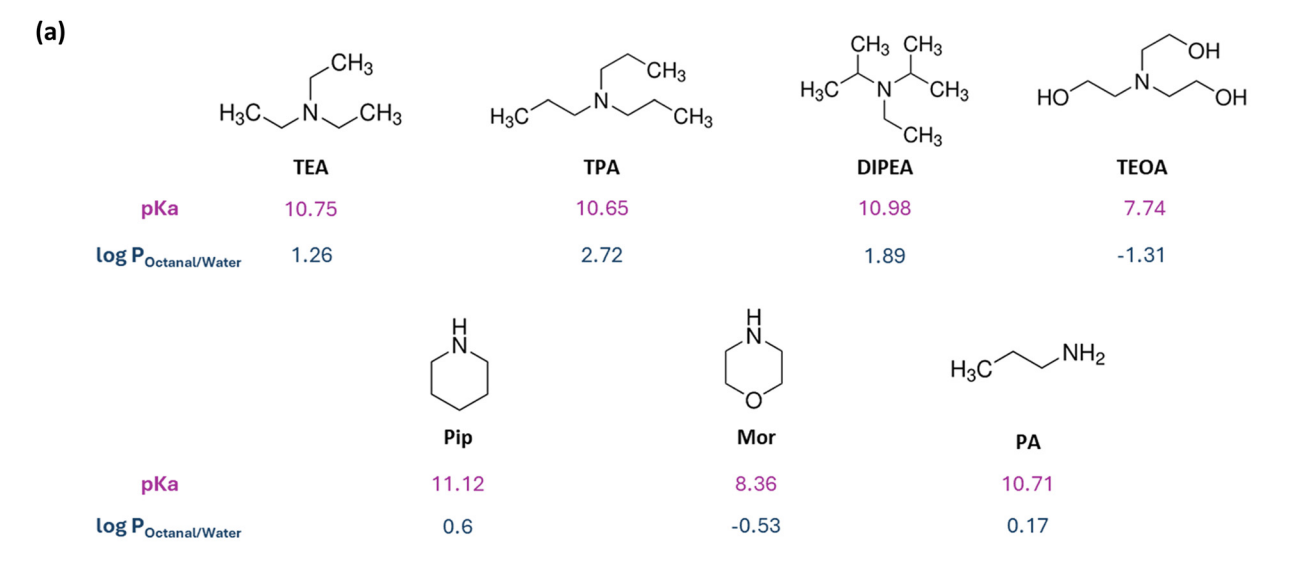


Fig. 5 A proposed mechanism for formate synthesis over Ru<sup>(III)</sup>@MCM in the presence of TEA.



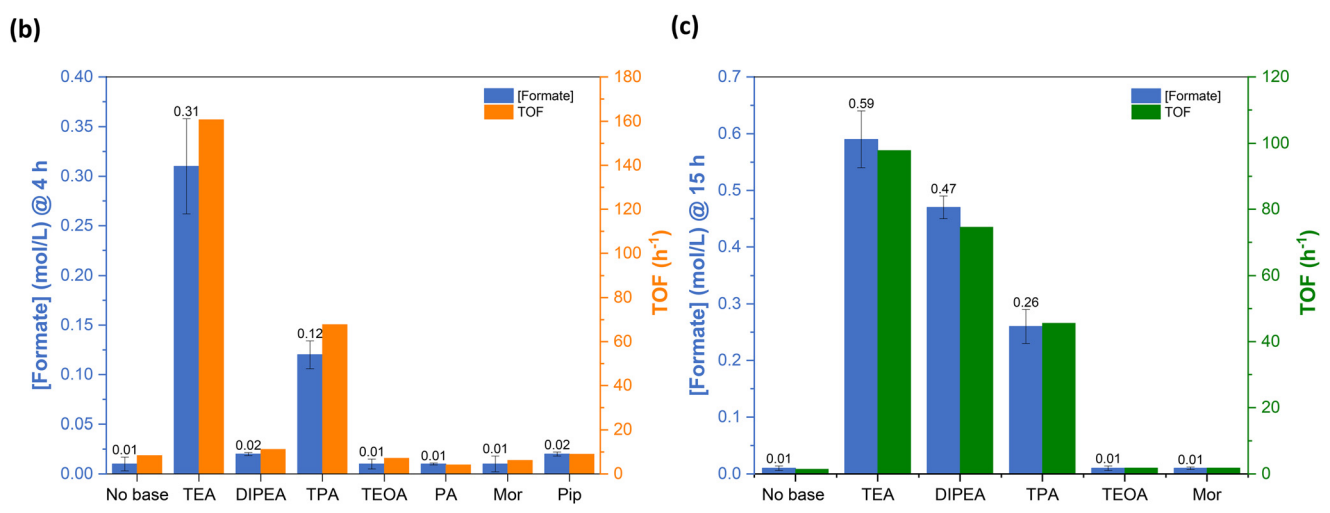


Fig. 6 Screening of amines with different basicity and lipophilicity. (a) for CO<sub>2</sub> hydrogenation to formate over Ru<sup>(III)</sup>@MCM (b) and Ru<sup>(III)</sup>@Mic (c). Conditions:  $3.1 \mu mol Ru$ , 9 mmol of amine, 4.5 mmol EtOH (b), 6 mL H<sub>2</sub>O, 30 bar H<sub>2</sub>, 20 bar CO<sub>2</sub>, 90 °C, 4 h (b) or 15 h (c).

metal site. Different tertiary, secondary and primary amines with varied basicity, lipophilic and steric properties (Table S6, SI, Fig. 6(a)) were screened for CO<sub>2</sub> hydrogenation over Ru<sup>(III)</sup> @MCM, and their performance compared to that of TEA (Fig. 6(b)). Lipophilicity was evaluated based on the partition coefficient between *n*-octanal and water  $(\log P_{\text{Octanal/Water}})$ , chosen as a model system to mimic the hydrophobic environment within the pores of Ru<sup>(III)</sup> (a)MCM and the aqueous phase.

TEA combines high basicity (p $K_a = 10.75$ ), moderate lipophilicity ( $log P_{Octanal/Water} = 1.26$ ), and low steric hindrance, and consequently exhibited the strongest promoting effect on formate production among all amines tested (Fig. 6(b)). TPA has a similar basicity to TEA and is more lipophilic (log Poctanal/Water = 2.72), but its bulkier alkyl chains likely hinder diffusion or orientation within the confined pore environment, resulting in approximately 3-fold lower activity. Interestingly, while both

DIPEA and TEOA are tertiary amines, they were nearly inactive, comparable to the control reaction without base. This highlights that tertiary structure alone is not sufficient for promotion. DIPEA is strongly basic (p $K_a = 10.98$ ) and fairly lipophilic ( $log P_{Octanal/Water} = 1.89$ ), but its significant steric bulk -arising from branched isopropyl groups—likely hinders its diffusion through the catalyst pores, resulting in poor performance. In contrast, TEOA has lower basicity (p $K_a = 7.74$ ) and is highly hydrophilic ( $log P_{Octanal/Water} = -1.31$ ), though it is small and sterically unhindered. These findings indicate that an optimal combination of strong basicity, intermediate lipophilicity, and minimal steric hindrance is essential to facilitate efficient base promotion within this catalytic system.

To evaluate to which extent poor pore accessibility as result of the bulkier nature of DIPEA might influence formate production, the same tertiary amines were screened over Ru(III) (a)Mic (Fig. 6(c)). In these conditions, DIPEA outperformed TPA.

The higher TOF of Ru<sup>(III)</sup>@MCM compared to Ru<sup>(III)</sup>@Mic can be a result of the increased electron density around the metal ion, promoted by the interaction with the supporting silica matrix.

Finally, screening secondary and primary amines, within the same range of  $pK_a$ ,  $^{8-11}$  led to productivities ten to twenty times lower than tertiary amines. Since secondary and primary amines typically react with  $CO_2$  to form stable carbamates, we hypothesize these species are less reactive over  $Ru^{(III)}$ @MCM.

# 4. Conclusions

The study of the liquid phase kinetics of CO<sub>2</sub> hydrogenation to formate over Ru<sup>(III)</sup>@MCM provides a deeper understanding of the reaction's dependence on H<sub>2</sub> partial pressure, concentration of TEA, pH, choice of solvent and role of the base.

The observed quasi second-order dependence in H<sub>2</sub> partial pressure reveals the importance of hydrogen activation for the reaction. High initial concentrations of TEA prevent the reaction because the high alkalinity of the medium favors formation of  $CO_3^{2^-}$  over  $HCO_3^-$ . Performing the reaction in water guarantees  $HCO_3^-$  formation over carbamates and maintaining a pH between 8–9 is crucial to keep  $HCO_3^-$  as the predominant species, ensuring formate synthesis over Ru<sup>(III)</sup>@MCM.

 $H_2$ – $D_2$  isotope scrambling confirms that the catalyst is able to activate  $H_2$ , with the addition of a TEA significantly enhancing formate production. Among the amines screened, TEA has the highest promoting effect. The presence of a base in the vicinity of the  $Ru^{(III)}$  active centers is crucial for  $H_2$  heterolytic dissociation during reaction. Small bases, with a moderate lipophilicity and a  $pK_a$  above 10 are preferred as promoters.

These findings provide insights into the role of bases in  $CO_2$  hydrogenation over  $Ru^{(III)}$ @MCM and guide optimization strategies for selective, base-free formic acid synthesis.

#### Author contributions

Catarina M. De Brito Mendes: conceptualization, investigation, formal analysis, validation, visualization, writing – original draft, writing – review and editing. Javiera Rubio: investigation. Francisca Rebelo: investigation. Sara Santos: investigation. Jan Öner: writing – review and editing. Vitaly V. Ordomsky: writing – review and editing. Mark Saeys: conceptualization, funding acquisition, project administration, supervision, writing – review & editing.

# Conflicts of interest

There are no conflicts of interest to declare.

# Data availability

Supplementary information is available. See DOI: https://doi.org/10.1039/D5CY00662G.

The processed data supporting this article (<sup>1</sup>H NMR and MS) has been included as part of the SI. Raw data are available on request from the corresponding author.

# Acknowledgements

This research was supported by the Energy Transition Fund, an initiative from the Belgian FPS Economy, under the Molecules at Sea (MuSE) project. The author V. V. O. acknowledges the financial support of the French National Research Agency (DEZECO, Ref. ANR-22- CE05-0005).

### References

- 1 J. Eppinger and K.-W. Huang, Formic Acid as a Hydrogen Energy Carrier, ACS Energy Lett., 2017, 2(1), 188–195.
- 2 K. Grubel, H. Jeong, C. W. Yoon and T. Autrey, Challenges and opportunities for using formate to store, transport, and use hydrogen, *J. Energy Chem.*, 2020, **41**, 216–224.
- 3 S. Chatterjee, I. Dutta, Y. Lum, Z. Lai and K.-W. Huang, Enabling storage and utilization of low-carbon electricity: power to formic acid, *Energy Environ. Sci.*, 2021, **14**(3), 1194–1246.
- 4 W. Leitner, Carbon dioxide as a raw material: the synthesis of formic acid and its derivatives from CO<sub>2</sub>, *Angew. Chem., Int. Ed. Engl.*, 1995, 34(20), 2207–2221.
- 5 R. Sun, Y. Liao, S.-T. Bai, M. Zheng, C. Zhou and T. Zhang, et al., Heterogeneous catalysts for CO<sub>2</sub> hydrogenation to formic acid/formate: from nanoscale to single atom, Energy Environ. Sci., 2021, 14(3), 1247–1285.
- 6 K. Rohmann, J. Kothe, M. W. Haenel, U. Englert, M. Hölscher and W. Leitner, Hydrogenation of CO<sub>2</sub> to Formic Acid with a Highly Active Ruthenium Acriphos Complex in DMSO and DMSO/Water, Angew. Chem., Int. Ed., 2016, 55(31), 8966–8969.
- 7 J. B. Jakobsen, M. H. Rønne, K. Daasbjerg and T. Skrydstrup, Are Amines the Holy Grail for Facilitating CO<sub>2</sub> Reduction?, Angew. Chem., Int. Ed., 2021, 60(17), 9174–9179.
- 8 G. A. Filonenko, R. van Putten, E. N. Schulpen, E. J. M. Hensen and E. A. Pidko, Highly Efficient Reversible Hydrogenation of Carbon Dioxide to Formates Using a Ruthenium PNP-Pincer Catalyst, *ChemCatChem*, 2014, 6(6), 1526–1530.
- 9 K. S. Rawat, A. Mahata and B. Pathak, Catalytic Hydrogenation of CO<sub>2</sub> by Fe Complexes Containing Pendant Amines: Role of Water and Base, *J. Phys. Chem. C*, 2016, **120**(47), 26652–26662.
- 10 R. E. Siegel, S. Pattanayak and L. A. Berben, Reactive Capture of CO<sub>2</sub>: Opportunities and Challenges, *ACS Catal.*, 2023, 13(1), 766–784.
- 11 G. Kovács, G. Schubert, F. Joó and I. Pápai, Theoretical investigation of catalytic HCO3<sup>-</sup> hydrogenation in aqueous solutions, *Catal. Today*, 2006, 115(1), 53–60.
- 12 R. Zhang, R. Liu, F. Barzagli, M. G. Sanku, L. Ce and M. Xiao, CO<sub>2</sub> absorption in blended amine solvent: Speciation, equilibrium solubility and excessive property, *Chem. Eng. J.*, 2023, 466, 143279.
- 13 J. Kothandaraman, A. Goeppert, M. Czaun, G. A. Olah and G. K. Surya Prakash, CO<sub>2</sub> capture by amines in aqueous media and its subsequent conversion to formate with

- reusable ruthenium and iron catalysts, Green Chem., 2016, 18(21), 5831-5838.
- 14 T. Schaub and R. A. Paciello, A process for the synthesis of formic acid by CO<sub>2</sub> hydrogenation: thermodynamic aspects and the role of CO, Angew. Chem., Int. Ed., 2011, 32(50), 7278-7282.
- 15 K. R. Ehmann, A. Nisters, A. J. Vorholt and W. Leitner, Carbon Dioxide Hydrogenation to Formic Acid with Self-Separating Product and Recyclable Catalyst Phase, ChemCatChem, 2022, 14(19), e202200892.
- 16 C. Kim, K. Park, H. Lee, J. Im, D. Usosky and K. Tak, et al., Accelerating the net-zero economy with CO2-hydrogenated formic acid production: Process development and pilot plant demonstration, Joule, 2024, 8(3), 693-713.
- 17 O. Wang, C. M. De Brito Mendes, O. V. Safonova, W. Baaziz, C. A. Urbina-Blanco and D. Wu, et al., Tunable catalysis by reversible switching between Ru(III) single sites and Ru0 clusters in solid micelles, J. Catal., 2023, 426, 336-344.

- 18 O. Wang, S. Santos, C. A. Urbina-Blanco, W. Y. Hernández, M. Impéror-Clerc and E. I. Vovk, et al., Solid micellar Ru single-atom catalysts for the water-free hydrogenation of CO2 to formic acid, Appl. Catal., A, 2021, 290, 120036.
- 19 S. A. Burgess, A. M. Appel, J. C. Linehan and E. S. Wiedner, Changing the Mechanism for CO2 Hydrogenation Using Solvent-Dependent Thermodynamics, Angew. Chem., Int. Ed., 2017, 56(47), 15002-15005.
- 20 L. B. Hamdy, C. Goel, J. A. Rudd, A. R. Barron and E. Andreoli, The application of amine-based materials for carbon capture and utilisation: an overarching view, Mater. Adv., 2021, 2(18), 5843-5880.
- 21 D. B. G. Berry, I. Clegg, A. Codina, C. L. Lyall, J. P. Lowe and U. Hintermair, Convenient and accurate insight into solution-phase equilibria from FlowNMR titrations, React. Chem. Eng., 2022, 7(9), 2009-2024.